Geological and Geomorphological Controls on Rocky Shore Platforms: Insights from the Basque Coast, France

Contrôles géologiques et géomorphologiques sur les plates-formes côtières rocheuses : aperçu de la côte basque, France

Vincent Regard[1*], Grégoire M. Maillet[2], Philippe Razin[3], Adrien Dublanchet[1], Mélody Prémaillon[1,4], Thomas J. B. Dewez[4], Anne Briais[1,5], Anne Duperret[6], Clara Levy[4], Kevin Pedoja[7], Sébastien Baratchart[8], César Dyson[4], Nicole Guerrero[1], Yannick Thiery[4]

1- Géosciences Environnement Toulouse, Université de Toulouse, CNES, CNRS, IRD, UPS, 14 av. Edouard Belin, 31400 Toulouse, France

2- Univ Angers, Nantes Université, Le Mans Université, CNRS, Laboratoire de Planétologie et Géosciences, LPG UMR 6112, 49000 Angers, France

3- ENSEGID, UMR EPOC 5805, 1 allée Daguin 33607 Pessac, France

4- BRGM-French Geological Survey, F-45060 Orléans, France

5- Geo-Ocean, CNRS, Université de Brest, Ifremer, UMR6538, Rue Dumont d'Urville, 29280 Plouzané, France

6- UMR 6294 LOMC, CNRS, Université Le Havre Normandie, 53 rue de Prony, 76 600 Le Havre

7- Normandie Univ, Unicaen, Unirouen, CNRS, M2C, 14 000 Caen, France

8- Groupement d'Instrumentation Scientifique, Observatoire Midi Pyrénées, Université de Toulouse, CNES, CNRS, IRD, UPS, 14 av. Edouard Belin, 31400 Toulouse, France

This provisional PDF is the accepted version. The article should be cited as: BSGF - Earth Sciences Bulletin, https://doi.org/10.1051/bsgf/2026010

* Corresponding author: vincent.regard@get.omp.eu

Résumé

Les plates-formes rocheuses côtières forment une partie essentielle de l’espace côtier. Leur morphologie est issue de l'histoire géologique, de l'évolution du niveau de la mer ainsi que des processus d'érosion. Bien que la classification de Sunamura (1992) distingue trois types principaux de plates-formes (A, B, C), la morphologie détaillée de ces structures —en particulier la partie immergée — reste mal comprise, principalement en raison d'une accessibilité limitée. Dans cette étude, nous analysons les contrôles géologiques et géomorphologiques sur le développement des plates-formes rocheuses le long de la côte basque (France), à l’aide de données bathymétriques haute résolution acquises lors de la campagne SPLASHALIOT-1 (navire R/V Haliotis, 2014). Notre travail se concentre sur deux sites près de Saint-Jean-de-Luz : Socoa (un site de suivi à long terme de l’observatoire national Dynalit) et Kokotia, tous deux sous-tendus par des turbidites crétacées–paléogènes déformées lors de l’orogenèse pyrénéenne.

En combinant cartographie bathymétrique et observations géologiques, nous révélons que les deux sites présentent les caractéristiques d’une plate-forme de type A (au sens de Sunamura, 1992) : une surface plane, légèrement inclinée (1–2°), s’étendant sur 100 à 500 mètres au large. La morphologie de la plate-forme est fortement influencée par la stratification lithologique, les bancs de turbidites résistants façonnant la rugosité et les structures observées. Notamment, nous n’observons aucun escarpement au bas de l’estran ni plus loin en mer, ce qui remet en question l’hypothèse de l’ubiquité des rebords de bas estran dans les modèles d’évolution des côtes rocheuses.

La cartographie géologique prolonge la stratigraphie terrestre en mer, mettant en évidence des chevauchements et des failles normales (par exemple, la faille Bidart–Pointe Sainte Anne) qui compartimentent la plate-forme. Nos résultats suggèrent que la morphologie de la plate-forme enregistre principalement la stabilisation du niveau de la mer durant l'Holocène, avec peu de traces de niveaux (terrasses) plus anciens datant du dernier interglaciaire (MIS5). L'absence de ressauts ou de structures étagées marquées implique que les taux de recul des falaises (4–20 cm/an) n'ont pas permis préserver des morphologies plus anciennes.

Nous discutons également de la manière dont la rugosité structurale et les contrastes lithologiques modulent la dissipation de l'énergie des vagues, avec des implications pour le recul futur des falaises dans un contexte de montée du niveau de la mer. Cette étude souligne la nécessité de prendre en compte l'hétérogénéité géologique dans les modèles prédictifs d'évolution des côtes rocheuses.

Mots-clés : Plate-forme côtière rocheuse ; Bathymétrie ; Turbidites ; Niveau de la mer ; Dissipation de l'énergie des vagues ; Dynalit ; Recul des falaises côtières.

Abstract

Rocky shore platforms are critical coastal landforms whose morphology reflects the interplay between geological inheritance, sea-level history, and erosional processes. While Sunamura's (1992) classification distinguishes three main platform types (A, B, C), the detailed morphology of these features—especially their submerged components—remains poorly understood due to limited access. Here, we investigate the geological and geomorphological controls on shore platform development along the Basque Coast (France), using high-resolution bathymetric data acquired during the SPLASHALIOT-1 cruise (R/V Haliotis, 2014). Our study focuses on two sites near Saint-Jean-de-Luz: Socoa (a long-term monitoring site of the Dynalit national observatory) and Kokotia, both underlain by Cretaceous–Paleogene turbidites deformed during the Pyrenean orogeny.

By integrating bathymetric mapping, and geological observations, we reveal that both sites exhibit the characteristics of a Type A platform (sensu Sunamura, 1992): a planar, gently sloping surface (1–2°) extending 100–500 m offshore. The platform morphology is strongly influenced by lithological layering, with resistant turbidite beds shaping roughness and structural features. Notably, we observe no seaward cliff, challenging the hypothesis of ubiquity of low-tide cliffs in models of rocky coast evolution. Geological mapping extends onshore stratigraphy offshore, highlighting thrusts and normal faults (e.g., the Bidart–Pointe Sainte Anne Fault) that compartmentalize the platform.

Our results suggest that platform morphology primarily records Holocene sea-level stabilization, with limited evidence of deeper terraces from the Last Interglacial (MIS5). The absence of prominent scarps or stepped features implies that cliff retreat rates (4–20 cm/a) have been insufficient to preserve older morphologies. We further discuss how structural roughness and lithological contrasts modulate wave energy dissipation, with implications for future cliff retreat under sea-level rise. This study underscores the need to account for geological heterogeneity in predictive models of rocky coast evolution.

Keywords: Rocky shore platform; Bathymetry; Turbidites; Sea-level change; Wave energy dissipation; Dynalit; Seacliff retreat.

1. Introduction

Sunamura (1992) defined three general types of rocky shore ahead of a cliff: type A is a simple shore platform; type B is a platform with a seaward drop also called a seaward cliff or edge; and type C corresponds to a cliff with no platform. Apart from this basic and schematic classification, the morphology of platforms has largely remained unexplored (Trenhaile, 1980) due to the difficulty of accessing their underwater components (Kennedy, 2015). Advances in shallow bathymetry acquisition (e.g., Duperret et al., 2016; Kennedy, 2016) are filling this gap. These platform/cliff systems are known to result from the erosive action of the sea, which occurs primarily at elevations close to mean sea level (e.g., Lajoie et al., 1991; Trenhaile, 2008a). The morphology of the platform, as defined by Sunamura (1992), must therefore be shaped by the history of the sea's action, and in particular by its level. This results in a series of flat or gently sloping zones known as marine “terraces”. These terraces are believed to be the result of the sea carving out the rocks at these levels. This idea is supported by numerical modeling (e.g. Anderson et al., 1999; Trenhaile, 2014; Martinod et al., 2025) and by the observation and dating of sequences of raised terraces (e.g., Armijo et al., 1996; Perg et al., 2001; Saillard et al., 2011; Jara-Muñoz et al., 2015; Regard et al., 2017; Malatesta et al., 2022; Deiss et al., 2025). In contrast, in contexts of subsidence, reef terraces formed during a highstand are sometimes found in drowned positions (e.g., Woodroffe and Murray-Wallace, 2012; Puga-Bernabéu et al., 2016). Thus, the current state of a rocky coast is the result of morphogenesis over several periods, governed by variations in sea level.

During the last interglacial (often referred to as MIS5) , and particularly the last interglacial substage MIS 5e, the sea level stabilized three times at levels close to present day as emphasized by Cutler et al. (2003), Siddall et al. (2006), or Thompson and Goldstein (2006). These highstands are referred to as sea level highstands. These studies, along with the sea level curve (e.g. Spratt and Lisiecki, 2016) indicate that the main MIS5 highstand (MIS5e) lasted approximately 10 thousand years (ka) between 125 and 115 ka BP, reaching a level similar to the present-day one. Subsequent highstands occurred around 105 and 85 ka BP (MIS5c and MIS5a respectively), reaching levels 10 to 30 m below the present-day level, according to various assessments (Spratt and Lisiecki, 2016; de Gelder et al., 2022; Deiss et al., 2025). The study site corresponds to a stable area with negligible vertical movement. During the last climate cycle, the sea level was close to the current level during MIS5e, approximately 120 ka ago, and since MIS1, around 5 ka ago (Lambeck, 1997). It was slightly lower, around -10 to -20 m, during MIS5c, approximately 100 ka ago, and MIS5a, around 80 ka ago (Spratt and Lisiecki, 2016). According to the concepts reviewed above, the morphogenesis process must have unfolded as follows: (i) approximately 120 ka ago, the shore platform was actively carved out at a level that is roughly equivalent to current one; (ii) 100 and 80 ka ago, a slightly lower (10-20 m) platform was excavated, a process that may have erased the MIS5e platform completely or only in its distal part; and (iii) in the Holocene, the sea level was close to the current level (within 5 m, Lambeck, 1997), carving out a new platform by pushing back the cliff. Thus, we expect to find a step (cliff) in the lower part of the current platform. However, the existence of such a low-tide cliff is debated as a common feature along rocky coasts (e.g., de Lange and Moon, 2005; Moon and de Lange, 2008; Stephenson, 2008; Duguet et al., 2021).

The platform is traditionally understood as the place where the energy of incoming waves is dissipated. Thus, the morphology and depth of the platform influence the wave energy at the foot of the cliff (e.g. Anderson et al., 1999; Trenhaile, 2014; Matsumoto et al., 2024). As sea level rise leads to the platform becoming deeper below the water level, energy dissipation should decrease, consequently increasing wave energy at the foot of the cliff and accelerating cliff retreat (Shadrick et al., 2022). That said, this “average” effect is influenced by the fact that each platform will react differently depending on its morphology (e.g., slope, roughness, width, etc.) (Dickson et al., 2023; Matsumoto et al., 2024; Sous et al., 2025) and external forcing like tidal range (Trenhaile, 2008b) which may also evolve through time (Uehara et al., 2006). Dissipation of wave energy on platforms is complex and requires case studies that describe the morphology well in order to create predictive models (Sous et al., 2025). In this context, we focus on the morphology of the platform at a particular site in southwestern France.

I In this paper, we examine the morphology of the submarine shore platform near Saint-Jean-de-Luz along the Basque coast in France using a high-resolution (less than 1 m) bathymetry map acquired in June 2014 on the R/V Haliotis (Maillet, 2014). One part of the studied area, east of Socoa, is a long-term study site for the National Observation Service (SNO-Dynalit; www.dynalit.fr).The local shore platform was carved from sand and carbonate turbidites from the latest Cretaceous and early Paleogene periods. In addition to depicting the underwater morphology of the rocky coast, the new map clearly shows the geological bedding and structural deformation. We drew the offshore geological map using the bathymetry and geological observations along the coast (Razin, 1989). We finally interpreted the platform and rock shore morphology revealed by the bathymetry and geological maps in terms of carving episodes related to sea level variations.

The morphology of rocky coasts is shaped by a combination of various erosive processes as well as factors related to sea level. This study site allows us to address various questions regarding the morphological evolution of rocky coasts. (i) Can we identify the effects of the different highstands of the last interglacial? (ii) How does geological structure affect wave propagation and, consequently, the erosion of the foreshore and the cliff? Further research could investigate how the dissipation of wave energy on the foreshore might change as sea level rises, and whether this could lead to an increase in the rate of cliff retreat.

2. Geological and geomorphological settings

The Basque Coast is located southeast of the Bay of Biscay. The study area consists of two distinct zones on either side of the Bay of Saint Jean de Luz (**Figure 1**). and is only a part of the Basque Coast. The northern boundary is the Bidart sandy beach, and the southern boundary is Pointe Sainte Anne (Hendaye). The northeastern zone is two kilometers long and is called Kokotia, while the southwestern zone is five kilometers long and is called Socoa. The offshore extension of the study area is approximately 1.5 km.

2.1. Geology

The 30 km-long French Basque coast is rocky and characterized by cliffs of various turbidite and carbonate lithologies from the end of the Mesozoic and the beginning of the Cenozoic. These cliffs were affected by the Pyrenean orogeny (Razin, 1989). The study area comprises a section of the Basque coast characterized by a normal fault, the Bidart-Sainte Anne Fault (Razin, 1989), which trends roughly N60°E (in green in **Figure 1**). Using offshore data (bathymetry and sonar), Augris et al. (2009) confirmed Razin's (1989) finding that the faults outcropping at the Pointe Sainte Anne and Bidart are actually a single fault. Based on these observations, we drew the fault as a segment roughly parallel to the coastline in the study area (**Figure 1**). The Socoa area is a monocline that strikes 315–345°, dips 35–55° (Guillen, 2024), and is affected by northwest-trending strike-slip faults with a maximum offset of a few meters (**Figure 2**). The Kokotia zone is more deformed, as will be seen later.

The stratigraphic sequence of the study area, from Bidart to Hendaye (**Figure 1**), is mainly made up of carbonate gravity flows and hemipelagic deposits. These sediments accumulated in the deep Saint Jean de Luz basin, which is located between the Aquitanian carbonate platform and the southern margin of the future Massifs Basques (Razin, 1989; Mulder et al., 2009). The following lithologies can be found (**Table 1**), dated from the Cretaceous to the Eocene (Razin, 1989; Brusset et al., 1997; Genna et al., 2004): 700m-thick Guethary flintstone 'flysch' (Coniacian); ~350m-thick Socoa marl-calcareous 'flysch' (Coniacian-Santonian, outcropping along most of our study's coastline cf. **Figure 2**); 400m-thick Haizabia 'flysch' (Santonian-Campanian), itself subdivided into the Makila turbidites member (~300m) and Loya marl member (~90 m), including thick debris-flow deposits; tens of meters thick sandy Hendaye 'flysch' (Upper Campanian); Maastrichtian Bidart marls (120-190 m); 50m-thick pink Danian limestones; Selandian-Thanetian marls; and Ypresian Jaizkibel 'flysch'. These formations often show strong weathering near the Earth's surface. The weathered layer ("alterites") is thick above the calcareous lithologies around Guethary (up to 30 m thick) and thin (~2 m thick) above the marly formations to the southwest of Saint Jean de Luz Bay (Peter-Borie, 2008).

2.2. Hydrodynamic setting

The area is mesotidal, with a spring tide amplitude of 3.75 meters (SHOM, 2016). Waves primarily originate from the west-northwest. At the buoy location mentioned in **Figure 1**, they have an average height of 1.5 m and a period of 9.5 s (Abadie et al., 2005). The incoming wave direction is most often around N300°, with 7.5% of the waves being storm waves and 2% exceeding 4 m (Abadie et al., 2005).

2.3. Geomorphology

In terms of geomorphology, the turbidite layering significantly influences the shape of the cliffs. However, the rock platform at the base of the cliffs is generally flat (**Figure 2**), as is commonly observed (e.g., Trenhaile, 1999; Kennedy and Dickson, 2006; Moses and Robinson, 2011). The platform roughness is meter-scaled. During spring tides, the platform width extends approximately 100–150 meters. The cliffs are 20–40 meters high. They are highly weathered along the Kokotia shoreline. Little to no weathering is observed along the Socoa shoreline.

The rate of cliff recession has been estimated to be between 4 and 20 cm/yr based on a comparison of historical documents spanning 200 years (Aubié et al., 2005, 2011) and aerial photographs spanning 80 years (Martins et al., 2022). Cliff retreat rates vary due to rock lithological variations (Martins et al., 2022) and weathering (Aubié et al., 2005). The fastest retreats occur where weathering extends to the base of the cliff (Aubié et al., 2005, 2011). At the 700-meter-long Dynalit Socoa site in the eastern part of the Socoa zone, where alterites are absent, Martins et al. (2022) measured a cliff retreat rate of 4 cm/yr on aerial photographs taken over 80 years (1938–2018). Meanwhile, Prémaillon et al. (2021) measured moderate cliff recession values of 0.3–1.1 cm/yr on the same part of the coast based on a comparison of 3D data from aerial photographs taken over 54 years (1954–2008) and local photographs taken over 5.7 years (2011–2017). Although mean wave conditions are moderate, storm waves drive most of the mechanical work and platform erosion (Guillen, 2024).

Additionally, the rock formations that make up the cliffs may be susceptible to karstification (Genna et al., 2004), although little karstification has been observed besides on the cliff face itself. A drowned karst landscape has been reported offshore on Middle Eocene-Oligocene rocks (Vanara et al., 2007). These same rocks are visible and karstified near Biarritz.

Bilbao-Lasa et al. (2020) identified relics of submarine terraces carved into the bedrock, accompanied by numerous sea stacks, along the Spanish part of the Basque coast. These terraces have been linked to the history of the sea level after the Last Glacial Maximum (LGM). Six levels of terraces, ranging from -35 to -80 m, are particularly well documented (Bilbao-Lasa et al., 2020).

3. Data acquisition and processing

High-resolution shallow-water bathymetric data (**Figure 1**) were acquired during SPLASHALIOT-1 scientific cruise (V/O Haliotis, TGIR FOF - CNRS, IFREMER, IPEV, IRD) in 2014 (Maillet, 2014) using a Geoswath interferometric sonar (from GeoAcoustics), which was mounted on the ship's hull. The sonar operates at a frequency of 250 kHz in water depths up to 100 m, collecting bathymetric swaths with widths up to about five times the water depth. The resolution of the bathymetric grids in our study area is of the order of 1 m, and the vertical precision about 0.1 m. A Chirp sediment echosounder was used to investigate rare portions of the coast where sediments cover bedrock. Sediment characterization was also achieved by recording surface roughness using an ER60 single-beam echosounder coupled with the RoxAnn SACLAF system (Chivers, 1990) and by taking spot samples using a Van Veen grab. The vertical reference is the hydrological reference (2.174 m below the NGF reference level SHOM, 2016). Post-processing was performed using the Caraïbes software (Le Gal and Edy, 1997). Soundings were corrected for tide level and filtered to automatically remove unreliable data points, and further cleaned with manual picking of unreliable data points.

Two distinct areas were mapped to the southwest and northeast of the Bay of Saint-Jean-de-Luz: Socoa (**Figure 3**) and Kokotia (**Figure 4**), respectively. The bathymetry ranges from 1 to 40 meters below the zero level of the National Grid (NGF). Socoa covers 5.3 km² and extends from the Bay of Saint-Jean-de-Luz to the Bay of Loya (**Figure 3**). Kokotia covers 2.3 x 1.6 km² and faces the Lafitenia and Mayarco beaches (**Figure 4**).

The bathymetric maps are presented in **Figure 3** (Socoa) and **Figure 4** (Kokotia). We drew the salient relief lines from the bathymetry and its shading. These lines correspond to the more resistant layers, which are usually the C layers in the Bouma sequence (see Mulder et al., 2009; Prémaillon et al., 2021). Additional lines in the littoral zone are derived from aerial photographs, such as IGN orthophotographs from 2015 and the French government's Ortholittoral Project from 2000 and 2012, as well as Lidar topobathymetry (Litto3D, SHOM, 2023). These lines, along with the texture of the bathymetric relief, allow us to extrapolate the observed geology along the coast offshore. Additionally, we used the V-shaped cartographic representation of some beds to estimate the local dip using isohypses. These stratigraphic dips are recorded and reported on the geological map.

In the Socoa zone, we extrapolated the coastal geology, originally documented by Razin (1989), by tracing the stratigraphic layers from the coast to the open sea. We also leveraged the distinct textural signatures of the various lithological units, as observed in the bathymetric data (**Figure 5**). This process was straightforward along the Socoa segment (Corniche Basque), where the Socoa marl-calcareous 'flysch' and the Makila turbidites have undergone minimal deformation. However, the stratification observed on the coast indicates a fairly constant azimuth of the strata, except for the shear zones. Thus, extrapolation of the Socoa area can be done with a constant azimuth, as previously proposed by Razin (1989) and Genna et al. (2004). However, the offshore extension of lithostratigraphic units across the Kokotia area is uncertain, primarily due to the extensive sandy cover that obscures key geological features, as well as the more heavily deformed strata.

The data are available at: https://doi.org/10.6096/11003. They consist of bathymetric rasters, stratigraphic lines, and geological layer vectors (Regard, 2026).

4. Results

4.1. Offshore Geology

Figure 5 shows the geological map produced for the Socoa zone. From the Corniche Basque cliffs to the sea, the Socoa "flysch" and Makila turbidite units demonstrate a high degree of lateral continuity, providing strong evidence of their offshore extension. Further out to sea, the Hayzabia "flysch" and the Loya marls and limestones have less regular geometries and are not consistently parallel, with locally prominent overlaps. These relationships are interpreted as the surface expression of thrust structures previously described by Razin (1989). The thrusts were mapped by identifying duplicated stratigraphic layers and deviations from layer parallelism. These features were then correlated with thrusts observed in Loya Bay to the southwest by Razin (1989). Within the Hayzabia "flysch," several thrust branches were identified, likely reflecting duplex structures. These formations, together with the Hendaye "flysch" formation and the associated thrusts, are truncated by a structure subparallel to the coastline (**Figure 5**). At Pointe Sainte Anne, Razin (1989) interpreted this structure as a north-dipping normal fault. We agree with this interpretation and view the observed offshore contact as the continuation of the same normal fault. Above this fault, we identified a succession of layers attributed to the Bidart marls, the pink limestones, the Selandian-Thanetian marls, and finally, the Jaizkibel "flysch." Within this upper sequence, surface morphological expression is generally subdued, resulting in only moderate confidence in the mapping. The Jaizkibel "flysch" is an exception because it forms more prominent, clearly expressed relief. The Pointe Sainte Anne normal fault appears to truncate most of the stratigraphic sequence to the northeast of the Socoa zone, including the thrust structures. Below the thrust system, the bedding dip remains relatively consistent, while deformation becomes more pronounced in the younger units above the Hayzabia "flysch" decollement.

In Kokotia, the structural observations are not accurate enough for extrapolating the onshore geology to the offshore area and creating a geological map. Nevertheless, a clear zonation is observed (**Figure 4**). For the first ~400 m from the shore (bathymetry 0–10 m), a fairly regular layering pattern is observed whose texture resembles that of the Socoa "flysch" and Makila turbidites in the Socoa study area. For the next 800 m, the layers are disturbed, though some thick layers are visible. These are comparable to the Hayzabia "flysch" and the Loya marls and limestones. Northwest of the swath profiles (**Figure 4**), oceanward, a new parallel layering is found that we cannot confidently associate with any of the lithological series mapped in **Figure 5**. This layering has a texture characterized by relatively thick layers with fractures. This layering is relatively similar to the Jaizkibel 'flysch' or the Loya marls and limestones, but it is more likely related to the Bidart marls. The Bidart marls can be found in the hanging wall of the Bidart-Pointe Sainte Anne fault in Bidart, to the east.

4.2. Geomorphology

From a morphological perspective, both the Socoa and Kokotia zones exhibit relatively simple seafloor geometries. The morphology in Socoa is roughly equivalent from east to west, whereas it is more complex in Kokotia. To illustrate the shore-normal morphology, we calculated representative swath topographic profiles, showing statistics for the entire bathymetry raster along the boxes in **Figure 3** and **Figure 4**. **Figure 6** shows that these profiles exhibit little dispersion, indicating the continuity of the structures parallel to the shore. No prominent scarps are revealed. Instead, each profile can be divided into two distinct domains. The nearshore domain consists of a planar rocky shore platform with a gentle slope of no more than two degrees (1.85° and 0.85° in Socoa and Kokotia, respectively; see **Figure 6**). Further offshore, the slope decreases and the morphology becomes less planar. In Socoa, the transition between these two domains corresponds to the high-relief Hayzabia 'flysch', located at a water depth of approximately 20 m (**Figure 6**). In Kokotia, the transition appears to correspond to a change from a relatively monotonous stratigraphic series to more deformed units. This boundary likely corresponds to the Hayzabia 'flysch', which is observed at a water depth of approximately 10 m in Kokotia (**Figure 6**).

The Socoa area has little sand, except for the area closest to the shore. Kokotia's offshore area is mostly covered in sand, as is the nearshore area. This, coupled with deformation, complicates structure interpretation. As highlighted by Lerma et al. (2020), the presence and dynamics of these sandy deposits, coupled with deformation, can significantly impact the exposure of rocky platforms and complicate the interpretation of underlying geological structures.

5. Discussion

The objective of this study is to examine the primary processes that determine the morphology of the shore platform in a specific area of the French Basque Coast. Our observations were twofold: First, we examined the geological features, particularly the structural aspects. Second, we examined the geomorphological features to facilitate a more profound comprehension of wave modification over the shore platform, a subject to be explored in a subsequent study.

5.1. Offshore geology

From a geological perspective, the bathymetry makes it easy to identify the strata and associated deformations. The lithostratigraphic layers can be distinguished by their wavelength and texture. In the southwestern part of the study area (Socoa), the monoclinal structure is defined by strictly parallel layers, at least in the lower strata, extending all the way to the Makila turbidites. The stratification trending N66° is roughly parallel to the coastline. In the northeastern part of the study area (Kokotia), the lower strata resemble those in Socoa despite the layers' significant deformation. The upper strata are deformed by thrusts parallel to the coastline and rooted in the Haizabia 'flysch'. The top of the sequence may be affected by the Bidart Pointe Sainte Anne normal fault. While the Bidart-Pointe Sainte Anne fault cannot be dated, it is posterior to the Middle Eocene compressional structures it cuts.

5.2. Geomorphology

From a geomorphological point of view, the bathymetry reveals a very regular littoral rock platform with a dip of one to two degrees despite the one-meter-scale stratification. The platform extends 400–500 meters to depths of 10 m (Kokotia) to 20 m (Socoa). Apart from the platform's simple overall shape, the lithological imprint is obvious as it develops over the Socoa and Makila 'flysch'. At the transition with the upper strata (Hayzabia 'flysch'), the planarity of the bathymetry is lost and the morphology becomes heterogeneous with no apparent cause. The rocks' response to erosion could be more heterogeneous unless the cause is found in marine processes. These processes could be associated with sandbanks or sea-level history, as proposed by Bilbao-Lasa et al. (2020).

The coastal platform described here aligns with Type A, as defined by Sunamura (1992). This classification is supported by two key observations. First, the platform lacks both a seaward cliff and any abrupt increase in slope, which are features typically present in Type B platforms. Instead, bathymetric data reveal a gradual transition from a nearshore planar surface to deeper morphologies. This transition is primarily characterized by flattening and changes in substrate roughness, rather than a distinct break in slope. Second, this morphological shift appears to be driven by lithology rather than active coastal processes. Notably, no significant abrupt change is observed between 60 and 600 meters from the coastal cliff that can be associated with the last interglacial cliff (de Lange and Moon, 2005; Duguet et al., 2021). The distance between that abrupt and the current cliff would correspond to the cliff retreat integrated over the Holocene highstand (since ~6 ka, Lambeck, 1997; Leorri et al., 2012; Regard et al., 2012). Extrapolating the current cliff retreat rates over the Holocene (1-10 cm/yr, Aubié et al., 2011; Prémaillon et al., 2021; Martins et al., 2022) would place this abrupt at 60-600 m. Finally, we note that there is no evidence of terrace levels at greater depths, unlike the observations by Bilbao-Lasa et al. (2020) slightly further west (e.g., T1 at -13 m or T2 at -30 m).

As previously mentioned, the turbidite layering significantly influences the shape of the shore platform. However, its general planar shape is a good example of what Bird (2000) calls a seaward-sloping shore platform. The structural architecture that runs parallel to the coastline significantly impacts hydrodynamics. For example, the cross-shore water current toward the shore is balanced by an along-shore current located between hard layers and troughs that are perpendicular to the shore. Wave breaking dynamics are also likely greatly impacted by turbidite layering. Currently, scientific research is investigating wave propagation on this seabed (e.g., Nuyts et al., 2023; Sous et al., 2025). This research will enable the modeling of the seabed under various sea-level change scenarios and help anticipate changes in wave energy at the cliff base and the rate of cliff retreat.

6. Conclusions

We acquired new, high-resolution, meter-scale data along the rocky Basque coast in the Socoa and Kokotia areas around the Bay of Saint-Jean-de-Luz. These data clearly reveal Type A morphology, as defined by Sunamura (1992). Beyond this primary information, the data remarkably depict the structural organization into easily recognizable strata and formations. This structural organization and resulting roughness enable us to: (i) create a previously unpublished geological map and (ii) demonstrate that this roughness must be considered in hydrodynamic analyses of wave energy dissipation above the rocky platform in order to determine the intensity of wave impact at the base of the cliffs, especially in the context of potential future sea-level rise.

Acknowledgements

This paper is primarily based on data, whose acquisition was funded by CNRS-INSU ("campagnes à la mer" and post-campaign funds) on board of the R/V Haliotis from the 'flotte océanographique française' (fof), with various supports from SNO Dynalit, OMP/UPS (BQR), the European FEDER project EZPONDA (2018 – 2022), the NVA Falaise project, the Haliotis crew and the BIAF and GET laboratories. We thank the Gobierno Vasco (Eusko Jaurlaritza / Gobierno Vasco) for sharing bathymetric data. We thank O. Vanderhaeghe and two anonymous reviewers for constructive comments.

7. References

Abadie, S., Butel, R., Dupuis, H., and Brière, C., 2005, Paramètres statistiques de la houle au large de la côte sud-aquitaine: Comptes Rendus Geoscience, v. 337, p. 769–776, doi:10.1016/j.crte.2005.03.012.

Anderson, R.S., Densmore, A.L., and Ellis, M.A., 1999, The generation and degradation of marine terraces: Basin Research, v. 11, p. 7–19.

Armijo, R., Meyer, B., King, G.C.P., Rigo, A., and Papanastassiou, D., 1996, Quaternary evolution of the Corinth Rift and its implications for the Late Cenozoic evolution of the Aegean: Geophys. J. Int., v. 126, p. 11–53.

Aubié, S., Genna, A., and Petitjean, J., 2005, Evolution historique du littoral basque français: Observatoire de la côte Aquitaine, BRGM.

Aubié, S., Mallet, C., and Favennec, J., 2011, Caractérisation de l'aléa érosion (2020-2040) dela Côte Aquitaine dans le cadre de l'étude stratégique de gestion du trait de côte.: Observatoire de la côte Aquitaine, BRGM BRGM/RP-59095-FR, 98 p.

Augris, C., Caill-Milly, N., and de Casamajor, M.-N., 2009, Atlas thématique de l'environnement marin du Pays basque et du sud des Landes:

Augris, C., Cirac, P., Satra, C., and Mazé, J.-P., 1999, Le domaine marin côtier du Pays basque (Pyrénées-Atlantiques) - carte morpho-bathymétrique et carte des formations superficielles: IFREMER, http://www.quae.com/fr/r421-le-domaine-marin-cotier-du-pays-basque-pyrenees-atlantiques.html (accessed August 2016).

Bilbao-Lasa, P., Jara-Muñoz, J., Pedoja, K., Álvarez, I., Aranburu, A., Iriarte, E., and Galparsoro, I., 2020, Submerged Marine Terraces Identification and an Approach for Numerical Modeling the Sequence Formation in the Bay of Biscay (Northeastern Iberian Peninsula): Frontiers in Earth Science, v. 8, doi:10.3389/feart.2020.00047.

Bird, E., 2000, Coastal Geomorphology. An Introduction: Chichester, John Wiley & Sons.

Brusset, S., Déramond, J., and Souquet, P., 1997, Évolution tectono-sédimentaire des bassins flexuraux profonds et à taux de sédimentation réduit : exemple du bassin de flysch de Saint-Jean-de-Luz (Pyrénées-Atlantiques, France) au Crétacé supérieur: Comptes Rendus de l'Académie des Sciences - Series IIA - Earth and Planetary Science, v. 325, p. 265–271, doi:10.1016/S1251-8050(97)88299-7.

Chivers, R.C., 1990, New acoustic processing for underway surveying: The hydrographycal journal, v. 56, p. 9–17.

Cutler, K.B., Edwards, R.L., Taylor, F.W., Cheng, H., Adkins, J., Gallup, C.D., Cutler, P.M., Burr, G.S., and Bloom, A.L., 2003, Rapid sea-level fall and deep-ocean temperature change since the last interglacial period: Earth and Planetary Science Letters, v. 206, p. 253–271.

Deiss, N., Rohais, S., Regard, V., Armitage, J.J., Carretier, S., and Bonnet, S., 2025, Source-to-Sink Signal Propagation in a Small, Coupled Catchment-Deep-Sea Fan System: The Sithas Example From the Corinth Rift (Pleistocene, Greece): Basin Research, v. 37, doi:10.1111/bre.70044.

Dickson, M.E., Matsumoto, H., Stephenson, W.J., Swirad, Z.M., Thompson, C.F., and Young, A.P., 2023, Sea-level rise may not uniformly accelerate cliff erosion rates: Nature Communications, v. 14, p. 8485, doi:10.1038/s41467-023-44149-3.

Duguet, T., Duperret, A., Costa, S., Regard, V., and Maillet, G., 2021, Coastal chalk cliff retreat rates during the Holocene, inferred from submarine platform morphology and cosmogenic exposure along the Normandy coast (NW France): Marine Geology, v. 433, p. 106405, doi:10.1016/j.margeo.2020.106405.

Duperret, A., Raimbault, C., Le Gall, B., Authemayou, C., van Vliet-Lanoë, B., Regard, V., Dromelet, E., and Vandycke, S., 2016, High-resolution onshore–offshore morpho-bathymetric records of modern chalk and granitic shore platforms in NW France: Comptes Rendus Geoscience, v. 348, p. 422–431, doi:10.1016/j.crte.2015.06.005.

Eusko Jaurlaritza / Gobierno Vasco, 2009, Batimetrías marinas País Vasco. Año 2009:, https://www.osakidetza.euskadi.eus/batimetrias-marinas-pais-vasco-ano-2009/webosk00-sercon.

de Gelder, G., Husson, L., Pastier, A.-M., Fernández-Blanco, D., Pico, T., Chauveau, D., Authemayou, C., and Pedoja, K., 2022, High interstadial sea levels over the past 420ka from the Huon Peninsula, Papua New Guinea: Communications Earth & Environment, v. 3, p. 256, doi:10.1038/s43247-022-00583-7.

Genna, A., Capdeville, J.P., Mallet, C., and Deshayes, L., 2004, Etude géologique simplifiée de la Côte Basque: Observatoire de la côte Aquitaine, BRGM.

Guillen, L., 2024, Érosion des falaises de flysch du Pays Basque français: apports d'une approche typologique des instabilités gravitaires: Pau et Pays de l'Adour, 290 p., doi:10.70675/bd0afab6zad13z42d4z8a68z967fc0d9295b.

Jara-Muñoz, J., Melnick, D., Brill, D., and Strecker, M.R., 2015, Segmentation of the 2010 Maule Chile earthquake rupture from a joint analysis of uplifted marine terraces and seismic-cycle deformation patterns: Quaternary Science Reviews, v. 113, p. 171–192, doi:10.1016/j.quascirev.2015.01.005.

Kennedy, D.M., 2016, The subtidal morphology of microtidal shore platforms and its implication for wave dynamics on rocky coasts: Geomorphology, v. 268, p. 146–158, doi:10.1016/j.geomorph.2016.06.003.

Kennedy, D.M., 2015, Where is the seaward edge? A review and definition of shore platform morphology: Earth-Science Reviews, v. 147, p. 99–108, doi:10.1016/j.earscirev.2015.05.007.

Kennedy, D.M., and Dickson, M.E., 2006, Lithological control on the elevation of shore platforms in a microtidal setting: Earth Surface Processes And Landforms, v. 31, p. 1575–1584.

Lajoie, K.R., Ponti, D.J., Powell II, C.L., Mathieson, S.A., and Sarna-Wojcicki, A.M., 1991, Emergent marine strandlines and associated sediments, coastal California; a record of Quaternary sea-level fluctuations, vertical tectonic movements, climatic changes, and coastal processes, *in* Quaternary nonglacial geology: Conterminous U.S., Boulder, Colorado, Geological Society of America, The Geology of North America, v. K-2, p. 190–203.

Lambeck, K., 1997, Sea-Level change along the French Atlantic and Channel coasts since the time of the Last Glacial Maximum: Palaeogeog. Palaeoclim. Palaeoecol., v. 129, p. 1–22.

de Lange, W.P., and Moon, V.G., 2005, Estimating long-term cliff recession rates from shore platform widths: Engineering Geology, v. 80, p. 292.

Le Gal, J., and Edy, C., 1997, Caraïbes : un système de traitement de données de sondeurs multifaisceaux, *in* Proceedings of the 13th International Conference on Interactive Information and Processing Systems for Meteorology, Oceanography, and Hydrology, p. 284–287.

Leorri, E., Cearreta, A., and Milne, G., 2012, Field observations and modelling of Holocene sea-level changes in the southern Bay of Biscay: implication for understanding current rates of relative sea-level change and vertical land motion along the Atlantic coast of SW Europe: Quaternary Science Reviews, v. 42, p. 59–73, doi:10.1016/j.quascirev.2012.03.014.

Lerma, A.N., Paris, F., Garcin, M., and Dailloux, D., 2020, Sandy Stocks on a Rocky Coast: States and Monthly to Pluriannual Evolutions: Journal of Coastal Research, v. 95, p. 610–615, doi:10.2112/SI95-119.1.

Maillet, G., 2014, SPLASHALIOT-01 cruise, RV Haliotis:, doi:10.17600/14011400.

Malatesta, L.C., Finnegan, N.J., Huppert, K.L., and Carreño, E.I., 2022, The influence of rock uplift rate on the formation and preservation of individual marine terraces during multiple sea-level stands: Geology, v. 50, p. 101–105, doi:10.1130/G49245.1.

Martinod, J., Regard, V., Husson, L., and Carretier, S., 2025, Erosion, uplift, and terraces: Modelling the evolution of the Central Andes coastal topography: Geomorphology, v. 482, p. 109814, doi:10.1016/j.geomorph.2025.109814.

Martins, L., Thiery, Y., Guillen, L., Dewez, T., Lévy, C., and Garnier, C., 2022, Caractérisation spatiale et temporelle du recul du sommet de falaises basques : recherche méthodologique: Bulletin de l'association de géographes français. Géographies, v. 98, p. 421–439, doi:10.4000/bagf.8333.

Matsumoto, H., Dickson, M.E., Stephenson, W.J., Thompson, C.F., and Young, A.P., 2024, Modeling future cliff-front waves during sea level rise and implications for coastal cliff retreat rates: Scientific Reports, v. 14, p. 7810, doi:10.1038/s41598-024-57923-0.

Moon, V., and de Lange, W., 2008, Reply to the comment by Stephenson "Discussion of de Lange, W.P. and Moon, V.G. 2005. Estimating long-term cliff recession rates from shore platform widths. Engineering Geology 80, 292–301": Engineering Geology, v. 101, p. 292–294, doi:10.1016/j.enggeo.2008.04.007.

Moses, C., and Robinson, D., 2011, Chalk coast dynamics: Implications for understanding rock coast evolution: Earth-Science Reviews, v. 109, p. 63–73, doi:10.1016/j.earscirev.2011.08.003.

Mulder, T., Zaragosi, S., Razin, P., Grelaud, C., Lanfumey, V., and Bavoil, F., 2009, A new conceptual model for the deposition process of homogenite: Application to a cretaceous megaturbidite of the western Pyrenees (Basque region, SW France): Sedimentary Geology, v. 222, p. 263–273, doi:10.1016/j.sedgeo.2009.09.013.

Nuyts, S., Almar, R., Morichon, D., Dealbera, S., Abalia, A., Muñoz, J.M., Abessolo, G.O., and Regard, V., 2023, CoastCams: A MATLAB toolbox making accessible estimations of nearshore processes, mean water levels, and morphology from timestack images: Environmental Modelling & Software, v. 168, p. 105800, doi:10.1016/j.envsoft.2023.105800.

Perg, L.A., Anderson, R.S., and Finkel, R.C., 2001, Use of a new Be-10 and Al-26 inventory method to date marine terraces, Santa Cruz, California, USA: Geology, v. 29, p. 879–882.

Peter-Borie, M., 2008, Les massifs rocheux crétacés supérieurs du Labourd occidental : processus d'altération et instabilités littorales: Bordeaux 1, 369 p., http://www.theses.fr/2008BOR13732 (accessed August 2016).

Prémaillon, M., Dewez, T.J.B., Regard, V., Rosser, N.J., Carretier, S., and Guillen, L., 2021, Conceptual model of fracture-limited sea cliff erosion: Erosion of the seaward tilted flyschs of Socoa, Basque Country, France: Earth Surface Processes and Landforms, v. n/a, doi:10.1002/esp.5201.

Puga-Bernabéu, Á., Webster, J.M., Braga, J.C., Clague, D.A., Dutton, A., Eggins, S., Fallon, S., Jacobsen, G., Paduan, J.B., and Potts, D.C., 2016, Morphology and evolution of drowned carbonate terraces during the last two interglacial cycles, off Hilo, NE Hawaii: Marine Geology, v. 371, p. 57–81, doi:10.1016/j.margeo.2015.10.016.

Razin, P., 1989, Évolution tecto-sedimentaire alpine des Pyrénées basques À l'ouest de la transformante de Pamplona (Province de Labourd): Bordeaux III, 465 p.

Regard, V., 2026, Cote Basque. [dataset]. Getomatique:, doi:10.6096/11003.

Regard, V., Dewez, T., Bourlès, D.L., Anderson, R.S., Duperret, A., Costa, S., Leanni, L., Lasseur, E., Pedoja, K., and Maillet, G.M., 2012, Late Holocene seacliff retreat recorded by 10Be profiles across a coastal platform: Theory and example from the English Channel: Quaternary Geochronology, v. 11, p. 87–97, doi:10.1016/j.quageo.2012.02.027.

Regard, V., Pedoja, K., De La Torre, I., Saillard, M., Cortés-Aranda, J., and Nexer, M., 2017, Geometrical trends within sequences of Pleistocene marine terraces: selected examples from California, Peru, Chile and New-Zealand: Zeitschrift f??r Geomorphologie, v. 61, p. 53–73, doi:10.1127/zfg/2017/0389.

Saillard, M., Hall, S.R., Audin, L., Farber, D.L., Regard, V., and Hérail, G., 2011, Andean coastal uplift and active tectonics in southern Peru: 10Be surface exposure dating of differentially uplifted marine terrace sequences (San Juan de Marcona, ~ 15.4°S): Geomorphology, v. 128, p. 178–190, doi:10.1016/j.geomorph.2011.01.004.

Shadrick, J.R., Rood, D.H., Hurst, M.D., Piggott, M.D., Hebditch, B.G., Seal, A.J., and Wilcken, K.M., 2022, Sea-level rise will likely accelerate rock coast cliff retreat rates: Nature Communications, v. 13, p. 7005, doi:10.1038/s41467-022-34386-3.

SHOM, 2023, Partie maritime Litto3D® – Nouvelle- Aquitaine 2020-2022 (Licence ouverte/Open Data):, doi:https://doi.org/10.17183/L3D_MAR_AQT_2020_2022.

SHOM, 2016, Références Altimétriques Maritimes: SHOM.

Siddall, M., Chappell, J., and Potter, E.-K., 2006, Eustatic Sea Level During Past Interglacials, *in* The climate of past interglacials, Amsterdam, Elsevier, p. 75–92.

Sous, D., Pezerat, M., Dealbera, S., Michaud, H., and Morichon, D., 2025, Wave-driven amplification of surf-zone bottom stress on rough seabeds: Ocean Science, v. 21, p. 3165–3178, doi:10.5194/os-21-3165-2025.

Spratt, R.M., and Lisiecki, L.E., 2016, A Late Pleistocene sea level stack: Climate of the Past, v. 12, p. 1079–1092, doi:https://doi.org/10.5194/cp-12-1079-2016.

Stephenson, W., 2008, Discussion of de Lange, W. P. and Moon V. G. 2005. Estimating long-term cliff recession rates from shore platform widths. Engineering Geology 80, 292–301: Engineering Geology, v. 101, p. 288–291, doi:10.1016/j.enggeo.2008.04.008.

Sunamura, T., 1992, Geomorphology of Rocky Coasts: Chichester, UK, John Wiley & Sons.

Thompson, W.G., and Goldstein, S.L., 2006, A radiometric calibration of the SPECMAP timescale: Quaternary Science Reviews, v. 25, p. 3207–3215.

Trenhaile, A.S., 2008a, Modeling the role of weathering in shore platform development: Geomorphology, v. 94, p. 24–39.

Trenhaile, A., 2014, Modelling the effect of Pliocene–Quaternary changes in sea level on stable and tectonically active land masses: Earth Surface Processes and Landforms, v. 39, p. 1221–1235, doi:10.1002/esp.3574.

Trenhaile, A.S., 1980, Shore platforms: a neglected coastal feature: Progress in Physical Geography: Earth and Environment, v. 4, p. 1–23, doi:10.1177/030913338000400101.

Trenhaile, A.S., 2008b, The development of subhorizontal shore platforms by waves and weathering in microtidal environments: Zeitschrift Fur Geomorphologie, v. 52, p. 105–124.

Trenhaile, A.S., 1999, The Width of Shore Platforms in Britain, Canada, and Japan: Journal of Coastal Research, v. 15, p. 355–364.

Uehara, K., Scourse, J.D., Horsburgh, K.J., Lambeck, K., and Purcell, A.P., 2006, Tidal evolution of the northwest European shelf seas from the Last Glacial Maximum to the present: Journal of Geophysical Research, v. 111, doi:10.1029/2006JC003531.

Vanara, N., Perré, A., Pernet, M., Latapie, S., Jaillet, S., and Martine, O., 2007, Aroca (domaine marin côtier, Pays basque, France) : un karst continental ennoyé par les transgressions maritimes quaternaires: KARSTOLOGIA, v. 49, p. 43–55.

Woodroffe, C.D., and Murray-Wallace, C.V., 2012, Sea-level rise and coastal change: the past as a guide to the future: Quaternary Science Reviews, v. 54, p. 4–11, doi:10.1016/j.quascirev.2012.05.009.

Tables and Figure captions

Table 1. Stratigraphy of the study area

Formation	Age	Thickness (m)
Jaizkibel flysch	Ypresian	
Selandian-Thanetian marls	Selandian-Thanetian	
Danian pink limestones	Danian	50
Bidart marls	Maastrichtian	120-190
Hendaye flysch	Upper Campanian	
Haizabia flysch - Loya marls	Santonian-Campanian	90
Haizabia flysch - Makila turbidites	Santonian-Campanian	300
Socoa marl-calcareous flysch	Coniacian-Santonian	350
Guethary flintstone flysch	Coniacian	700

Figure 1. General map (B) of the French Basque Coast (see (A) for location). Aerial photos cover the onshore area; main localities and the Dynalit site are outlined. Arrows indicate the positions where the images in Figure 2 were taken. Shown in blue colors is the bathymetry acquired by Augris et al. (1999), with corresponding isobaths in meters (ellipsoid WGS84), completed to the west (thin lines) by isobaths provided by the regional government (ellipsoid ETRS89, Eusko Jaurlaritza / Gobierno Vasco, 2009). In blue to red colors is the newly acquired low-depth bathymetry (see thereunder for a zoom). Normal faults are drawn after the works by Augris (offshore domain; 2009) and Razin (onshore; 1989). Coordinates are in Lambert 93 (black in meters, top and right, crosses) and in degrees (blue, bottom and left, grid).

Figure 2. Two pictures of the turbidite-made cliff (30 m-high) and rocky shore platform (Socoa 'flysch'). The turbidite alternating layers (decameter to meter-thick) are highlighted by marine abrasion and reveals subtle deformations like meter-scale left-lateral shear in A. They have been shot from the eastern part of Socoa area in Figure 1. Photo A is looking to the ENE, while photo B is looking towards

the WSW (background is constituted first by Pointe Sainte Anne in Hendaye and then by Jaizkibel summit in Spain).

Figure 3. Bathymetry of Socoa study area with isobath contours (the vertical reference is the hydrological reference = 2.174 m below the NGF reference level SHOM, 2016) plus those from Augris et al. (1999, ellipsoid WGS84) revealing a good correspondence (blue). Similar projection as **Figure 1**. OpenStreetMap is used as background. A: map with line drawing of its low-wavelength relief. B. shows the raw map with the black box indicating the extent of the swath profile shown **Figure 6**.

Figure 4. Bathymetry of Kokotia study area (the vertical reference is the hydrological reference = 2.174 m below the NGF reference level SHOM, 2016) with isobath contours plus those from Augris et al. (1999, ellipsoid WGS84), revealing a good correspondence (blue). Similar projection as **Figure 1**. OpenStreetMap is used as background. The line drawing of the low-wavelength relief. B. shows the raw map with the black box indicating the extent of the swath profile shown **Figure 6**.

Figure 5. Geological map of the Socoa zone interpolated from outcrops at the coast and bathymetry relief. Background blue gradient map and dashed lines figure the bathymetry recorded by Augris et al. (2009).

Figure 6. Cross-shore swath profiles (top: 2125 m-wide Socoa swath profile, **Figure 3**, bottom: 465 m-wide Kokotia swath, **Figure 4**). Same altitudinal reference as Figure 3 (hydrological reference = 2.174 m below the NGF reference level SHOM, 2016) The nearshore slope is very regular. Its slope and width are, respectively, 1.85° and 500 m for Socoa (A) and 0.85° and 350 m for Kokotia (B). The nearshore

geology can be deduced from the bathymetrical data for Socoa. Offshore the Hayzabia flysch, it is not documented enough to be accurately drawn. Note there is no cliff at seaward platform edge.

Figures

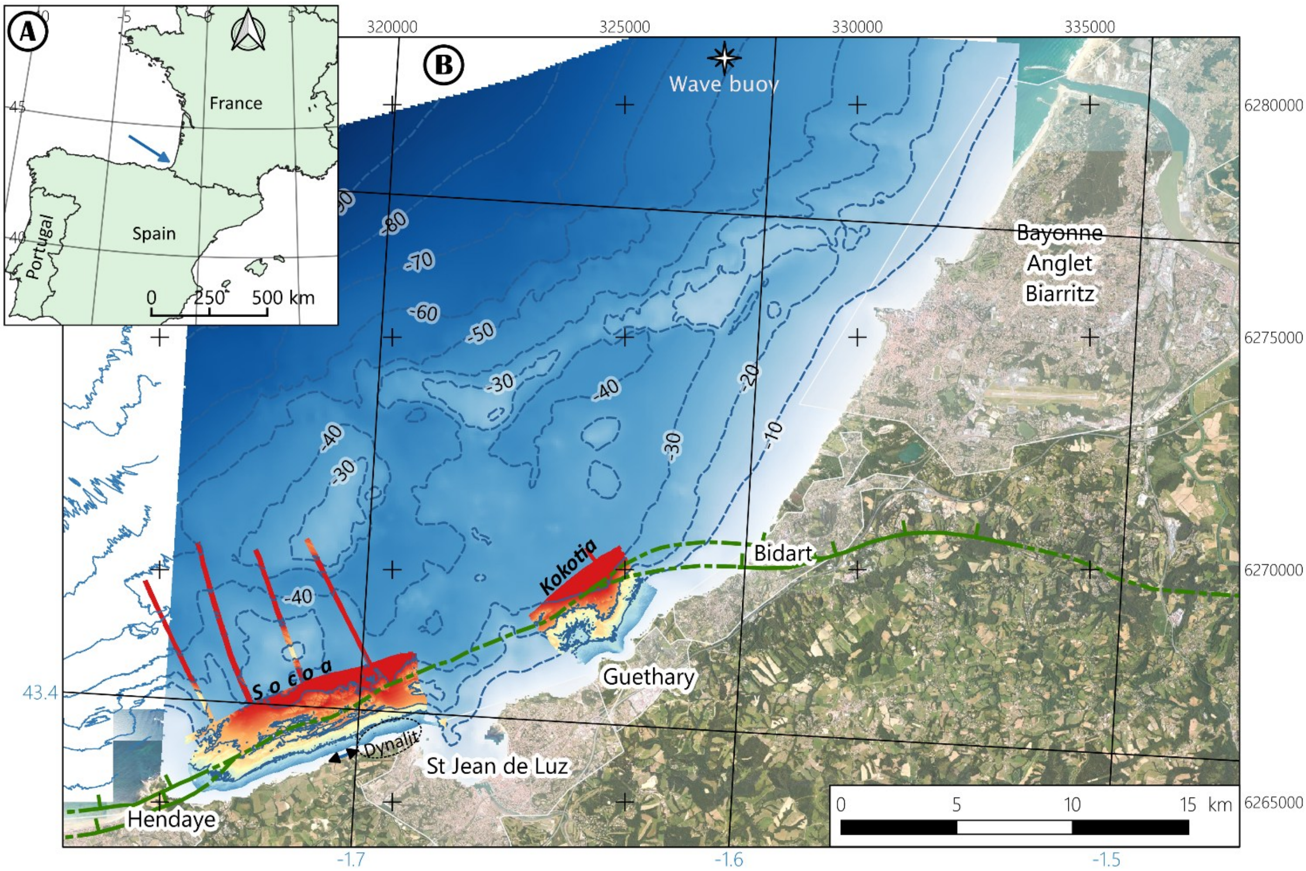

Figure 1.

Figure 2.

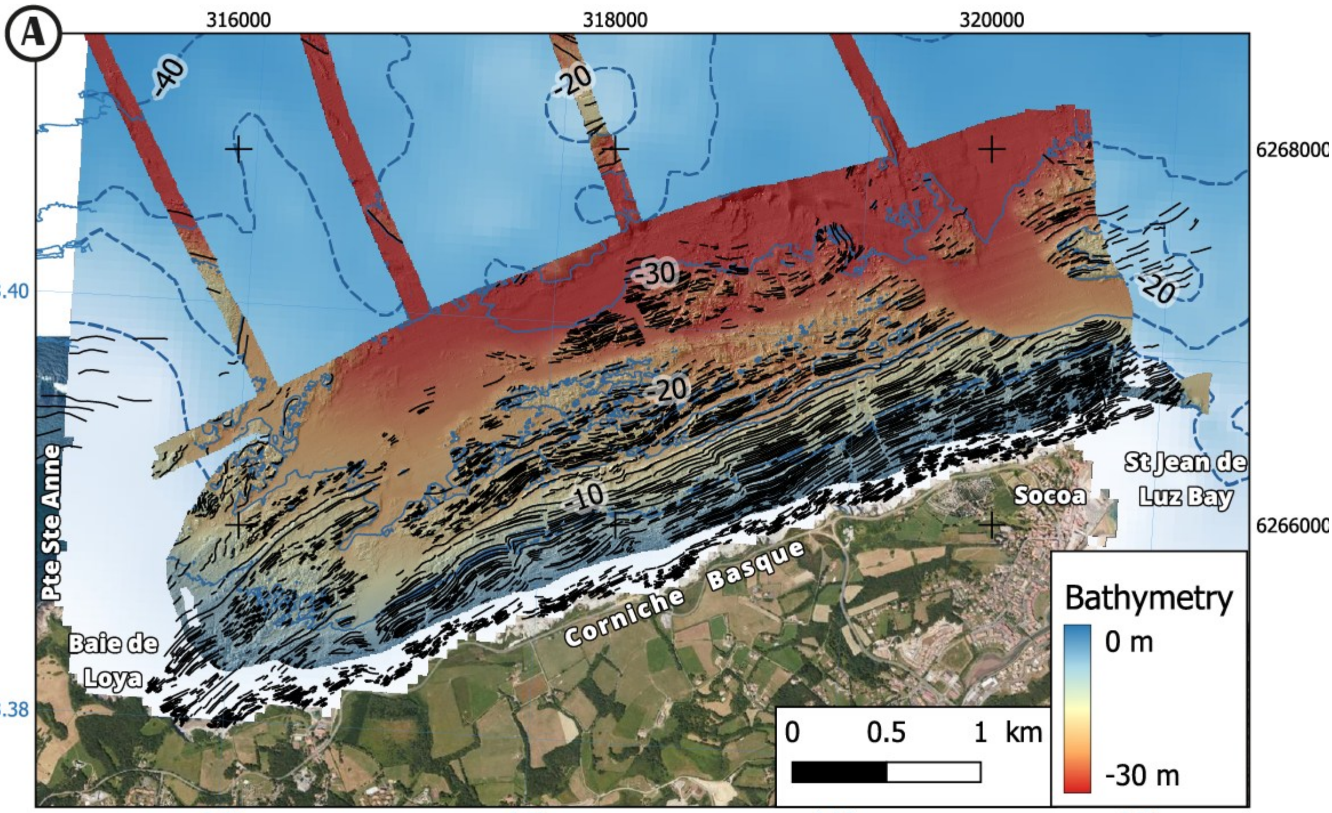
A
316000
318000
320000
6268000
6266000
43.40
43.38
-1.74
-1.72
-1.70
-1.68
-40
-20
-30
-20
-10
-20
Pte Ste Anne
Baie de Loya
Corniche Basque
Socoa
St Jean de Luz Bay
Bathymetry
0 m
-30 m
0 0.5 1 km

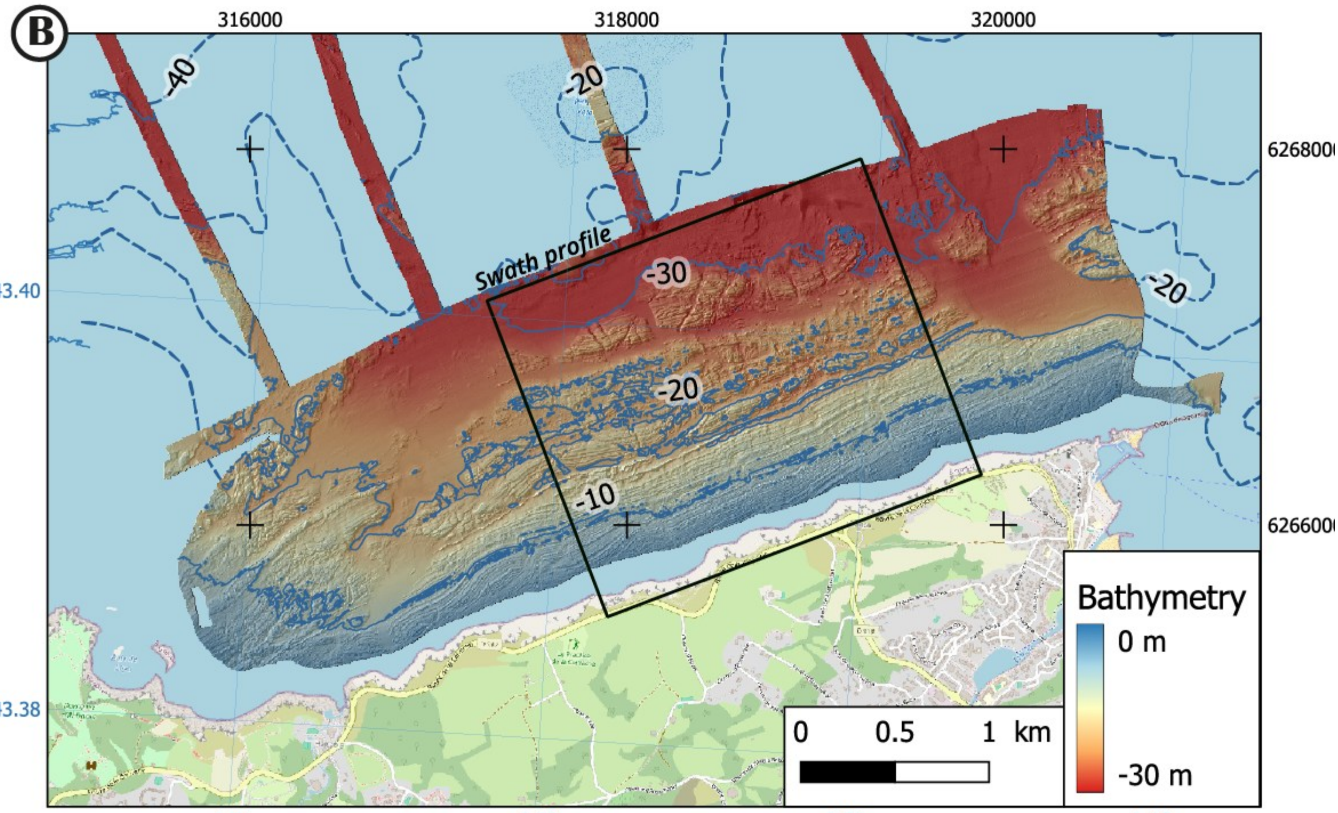
B
316000
318000
320000
43.40
43.38
-1.74
-1.72
-1.70
-1.68
-40
-20
Swath profile
-30
-20
-10
-20
Bathymetry
0 m
-30 m
0 0.5 1 km

Figure 3.

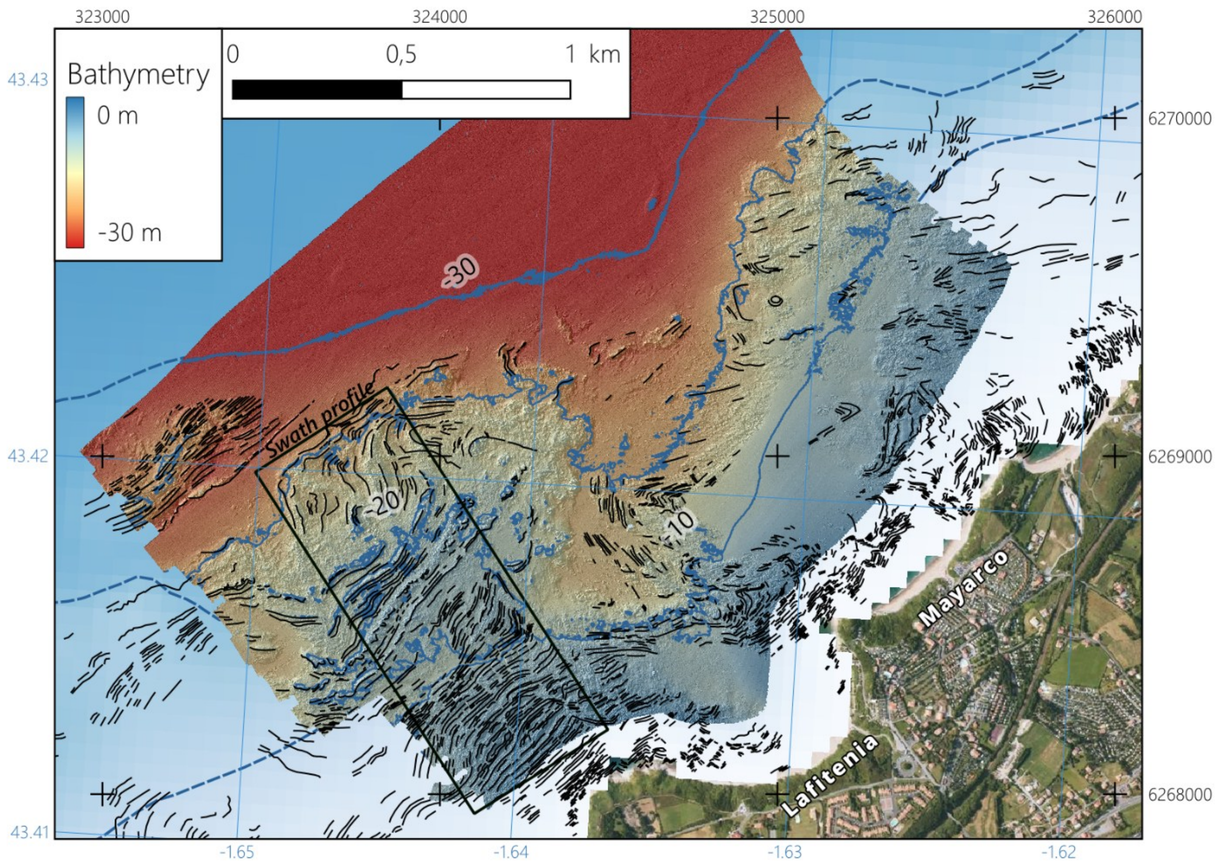

323000
324000
325000
326000
Bathymetry
0 m
-30 m
0
0,5
1 km
43.43
43.42
43.41
6270000
6269000
6268000
-30
-20
-10
Swath profile
Mayarco
Lafitenia
-1.65
-1.64
-1.63
-1.62

6__

Figure 4.

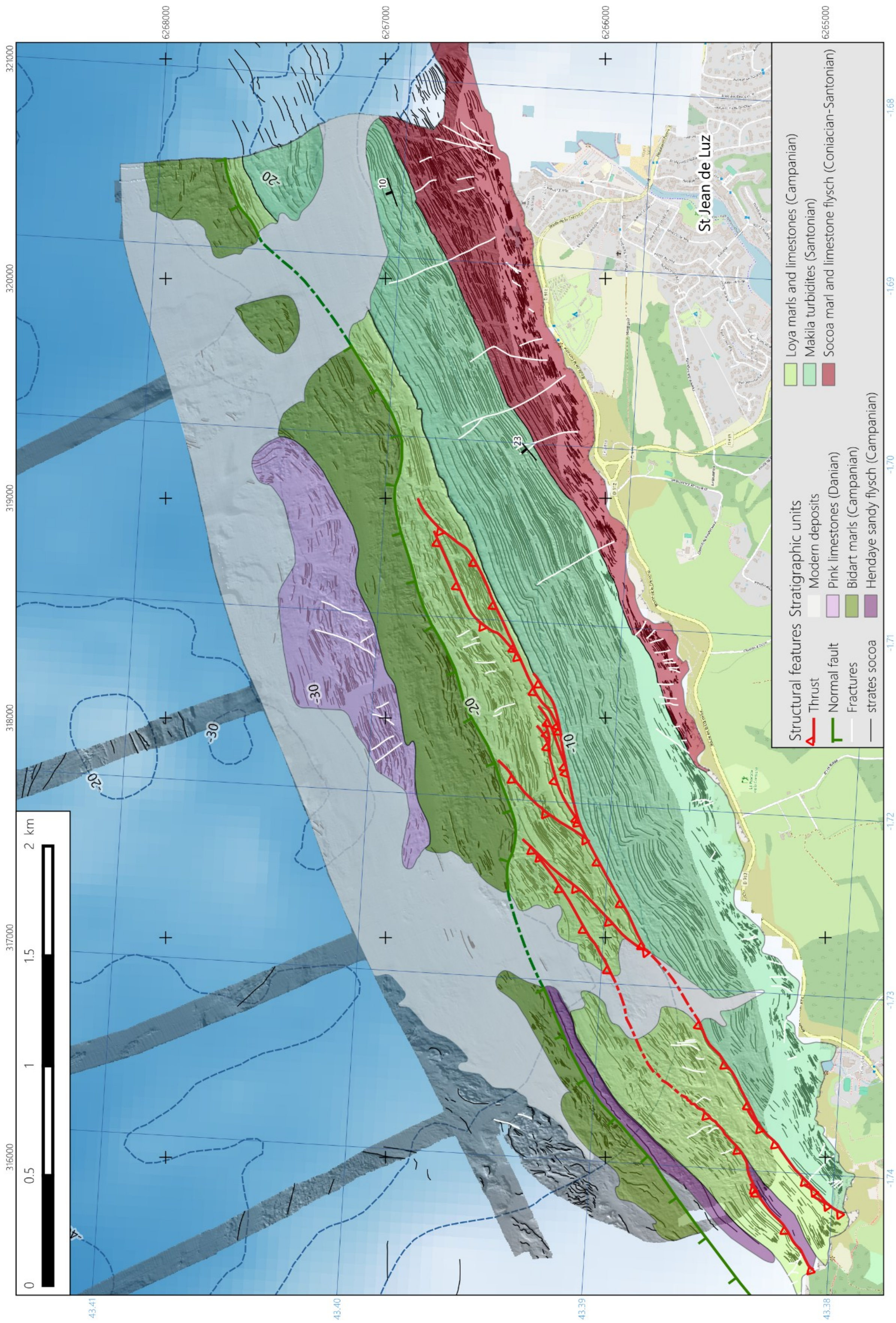

Structural features
Thrust
Normal fault
Fractures
strates socoa
Stratigraphic units
Modern deposits
Pink limestones (Danian)
Bidart marls (Campanian)
Hendaye sandy flysch (Campanian)
Loya marls and limestones (Campanian)
Makila turbidites (Santonian)
Socoa marl and limestone flysch (Coniacian-Santonian)
St Jean de Luz
0 0.5 1 1.5 2 km

Figure 5.

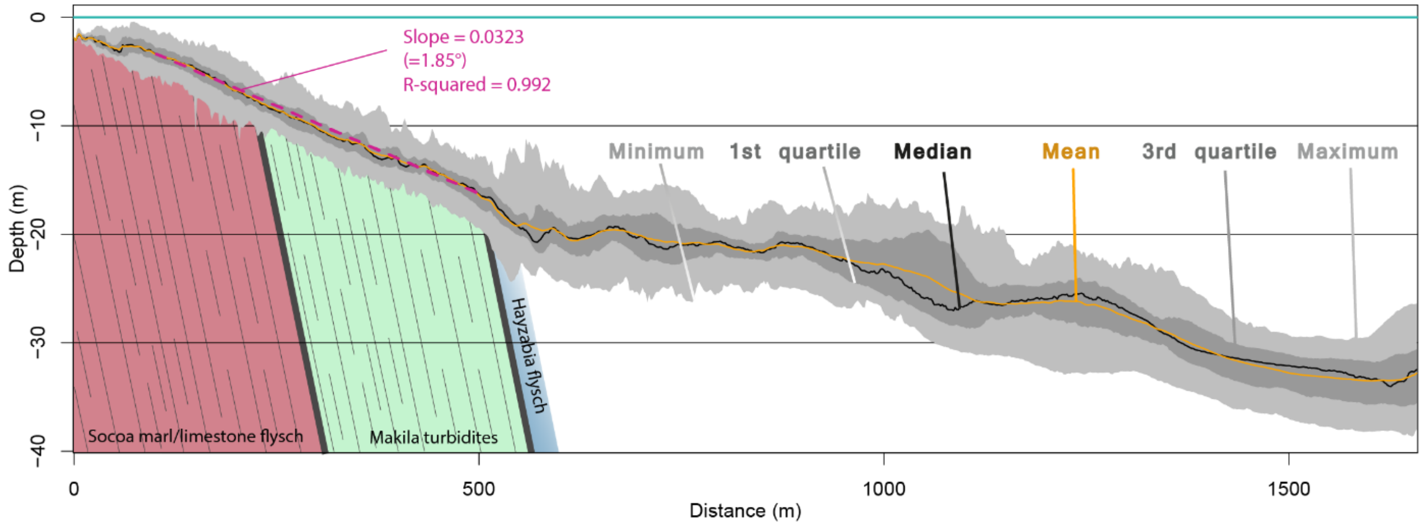

A) Socoa

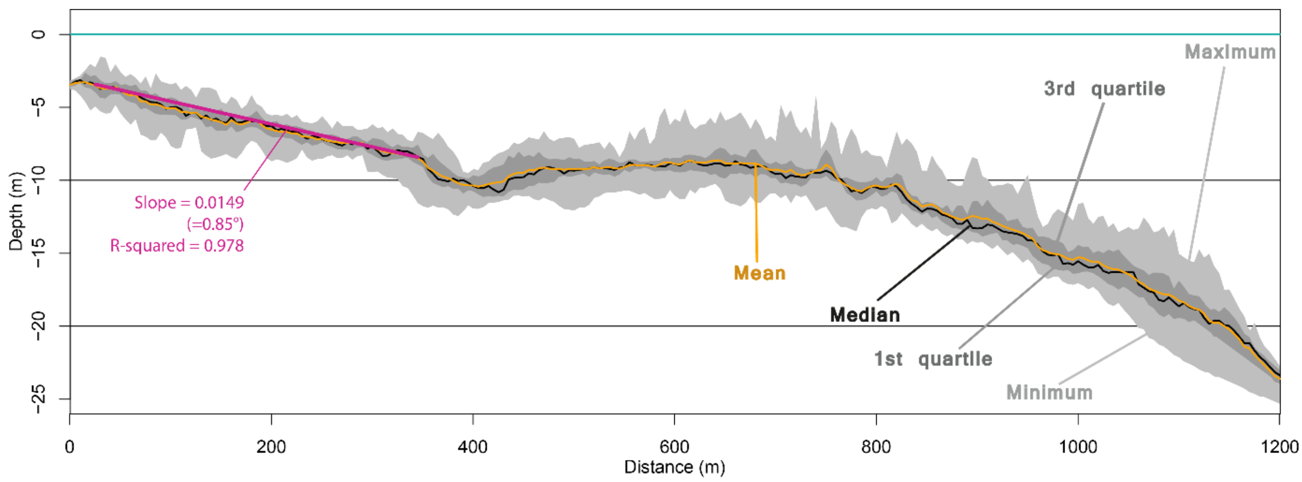

B) Kokotia

Figure 6.